

THE MUTUAL RADIATION IMPEDANCE EFFECT ON PHASED ARRAY

D. Mikami, T. Yokoyama, A. Hasegawa, T. Kikuchi

Dept. of Applied Physics, National Defense Academy, Yokosuka, Japan

1. INTRODUCTION

Recently, low frequency and high power underwater transducers are required, however, the interaction between array elements is not negligible in these transducers. This interaction effect, unless compensated for in the design, reduces the power output of a transducer array, and deteriorates its beam pattern.¹⁾ The source of this interaction is the existence of mutual radiation impedance between array elements. It could be that one of the elements of the array may work as a sink and absorbs the other element's power.¹⁾

A transducer vibrating in the medium gives action to the medium as it receives reaction from the medium. This reaction from the medium is called self radiation impedance. When there are two transducers vibrating closely side by side, the action of one transducer is conveyed to another transducer through the medium. These two transducers are acting against each other. Consequently, they get action from the other transducer in addition to self radiation impedance. This additional action is so called mutual radiation impedance.^{2), 3)}

Sound radiation and absorption by mutual radiation impedance may finally cause the destruction of the transducers.⁴⁾ From a different point of view however, this may be a fundamental theory of active sound control, which controls the noise source's power. Therefore, much research is being reported as of late, on this topic.

In this research, mutual radiation impedance of a sound source is numerically obtained and an overview of sound power radiation and absorption from underwater transducers is visually provided by a model experiment using a piezo-rubber hydrophone array.

2. THEORY

2.1 Calculation of the self radiation impedance

We assume two identical rectangular transducers of width a and height b in an infinite baffle, where d is the center-to-center distance between transducers (Fig.1). Transducer 1 vibrates with the effective velocity U_1 and angular frequency ω . The sound pressure $p(x, y)$ at the point $M(x, y)$ on transducer 1 caused by the motion of transducer 1 is given by

$$p(x, y) = \frac{j\rho ck}{2\pi} U_1 e^{j\omega t} \int_{S_1} \frac{e^{-jkr}}{r} dS_1, \quad (1)$$

where c is the sound velocity in the medium, ρ is the density of the medium, and k is the wave number. The force as reaction from the medium caused by the sound pressure of transducer 1 is given by

$$F_{11} = \int_{S_1} p(x, y) dS_1. \quad (2)$$

THE MUTUAL RADIATION IMPEDANCE EFFECT ON PHASED ARRAY

The self radiation impedance is given by

$$Z_{11} = \frac{F_{11}}{U_1 e^{j\alpha}} \quad (3)$$

2.2 Calculation of the mutual radiation impedance

The force to transducer 2 from the sound pressure (1) is given by

$$F_{21} = \int_{S_2} p(x, y) dS_2 \quad (4)$$

Then, the mutual impedance is given by

$$Z_{21} = \frac{F_{21}}{U_1 e^{j\alpha}} \quad (5)$$

The mutual impedance decreases as the distance between transducers increases. The distance is described by a non-dimensional number (ka), which is normalized by the wave number k and transducers size a .

2.3 Calculation of the total power output

Forces given to transducers 1 and 2 which are caused by the sound pressure of each transducer is given by⁵⁾

$$\begin{aligned} F_1 &= Z_{11}U_1 + Z_{12}U_2, \\ F_2 &= Z_{21}U_1 + Z_{22}U_2. \end{aligned} \quad (6)$$

And power outputs from transducers are given by

$$\begin{aligned} W_1 &= \frac{1}{2} \text{Re}[F_1 \cdot U_1^*], \\ W_2 &= \frac{1}{2} \text{Re}[F_2 \cdot U_2^*]. \end{aligned} \quad (7)$$

Consequently, the total power output from these two transducers are given by

$$W = W_1 + W_2 \quad (8)$$

Matrices are utilized in applying above formations to a realistic underwater transducer array. Then each power output from individual elements by each force are given by

$$\begin{bmatrix} \hat{F}_1 \\ \vdots \\ \hat{F}_i \\ \vdots \\ \hat{F}_L \end{bmatrix} = \begin{bmatrix} \hat{Z}_{11}\hat{U}_1 + \dots + \hat{Z}_{1j}\hat{U}_j + \dots + \hat{Z}_{1L}\hat{U}_L \\ \vdots \\ \hat{Z}_{i1}\hat{U}_1 + \dots + \hat{Z}_{ii}\hat{U}_i + \dots + \hat{Z}_{iL}\hat{U}_L \\ \vdots \\ \hat{Z}_{L1}\hat{U}_1 + \dots + \hat{Z}_{Lj}\hat{U}_j + \dots + \hat{Z}_{LL}\hat{U}_L \end{bmatrix} \quad (9)$$

$$W_i = \frac{1}{2} \text{Re}[F_i \cdot U_i^*] \quad (10)$$

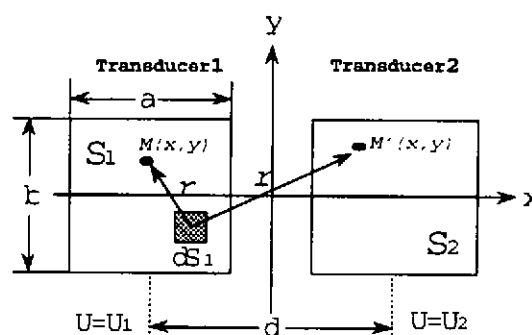


Fig.1 Coordinate system for mutual radiation impedance of two rectangular pistons.

THE MUTUAL RADIATION IMPEDANCE EFFECT ON PHASED ARRAY

$$W = \sum_{i=1}^I W_i \quad (11)$$

3. NUMERICAL ANALYSIS

Figure 2 shows the self and the mutual radiation impedances calculated for a square piston array. (a) shows the self radiation impedance of an element. (b) shows the mutual radiation impedance between elements located side by side. (c) shows the mutual radiation impedance between elements located diagonally. And (d) shows the mutual radiation impedance between elements located over an element. All impedances are characterized by ka .

4. APPARATUS AND MEASUREMENT

The hydrophone array for the model experiment was made of a piezo-rubber sheet. This piezo-rubber is a composite material of rubber and piezoelectric powder, which is sandwiched between conductive rubber electrodes (Fig.3). It is very flexible and easy to cut. Its mechanical Q in water equals to 4, which is low

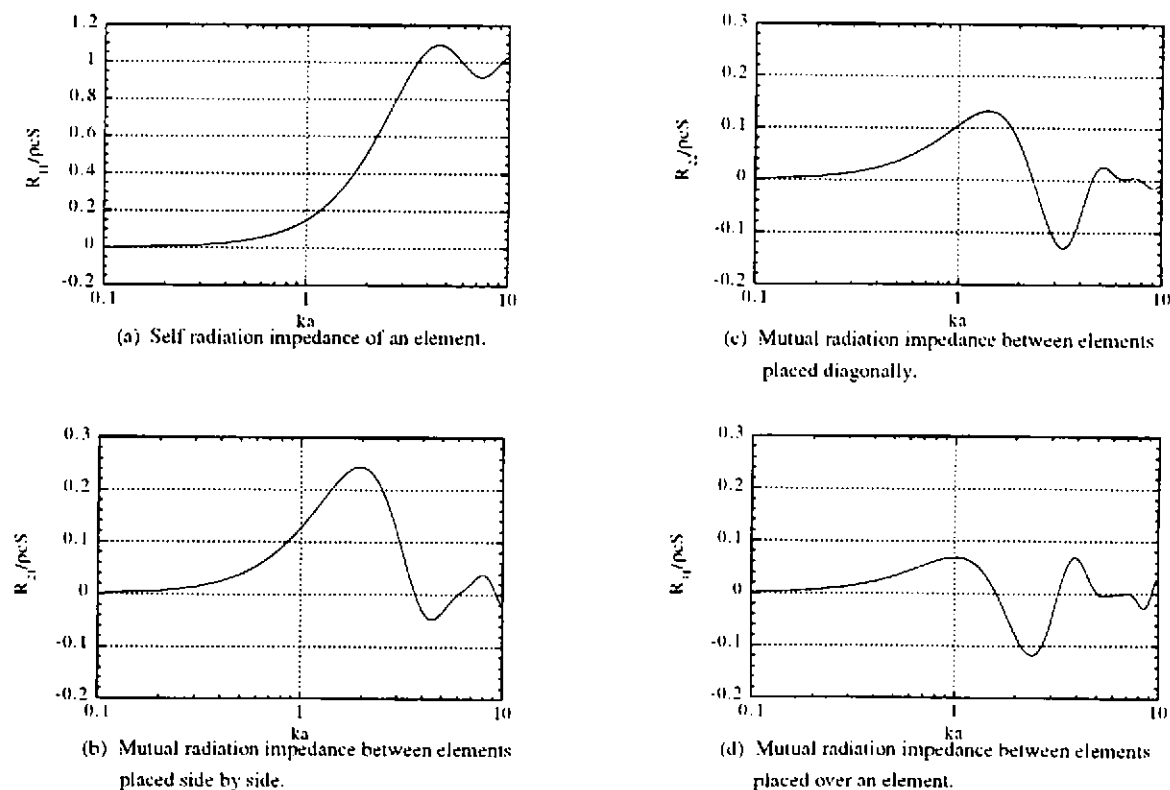


Fig.2 Self and mutual radiation impedance between elements of a rectangular piston array.

THE MUTUAL RADIATION IMPEDANCE EFFECT ON PHASED ARRAY

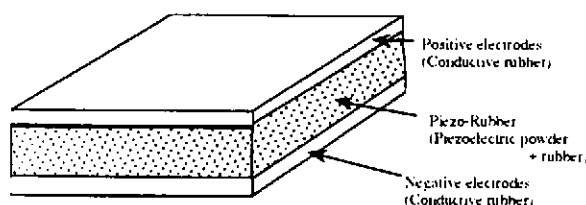


Fig.3 Piezo-electric rubber sheet.

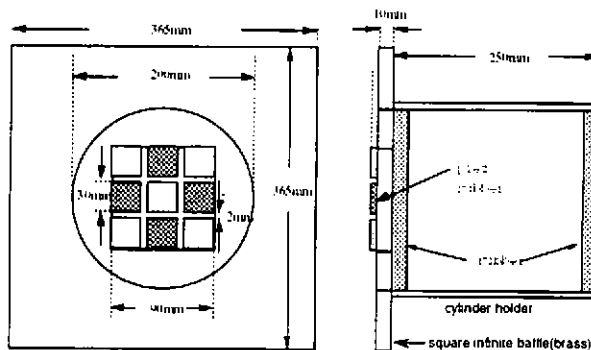


Fig.4 Transducer array made of piezo-rubber.

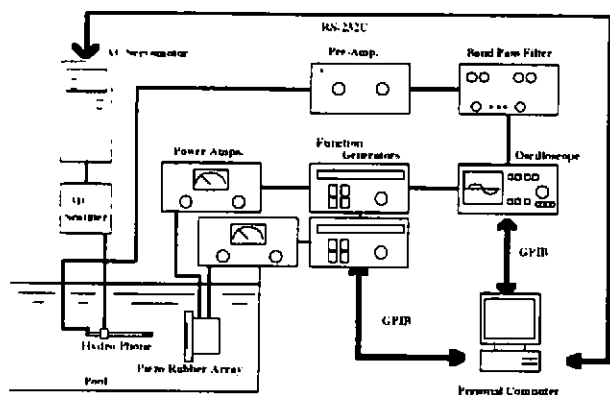


Fig.5 Block diagram of the measurement system.

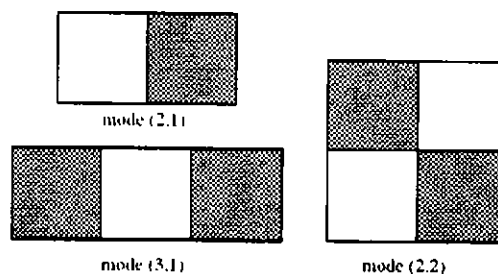


Fig.6 Patterns of array elements.

enough compared with a *Langevin* type PZT transducer. One array set therefore allows broad band frequency measurement. The apparatus consists of a 3×3 hydrophone array. One element has a dimension of $30 \times 30 \times 1\text{mm}$ (Fig.4).

The measurement was controlled automatically by a personal computer system shown on Fig.5. Complex sound pressures were measured on 2 planes separated from the array plane by 5mm and 15mm. Each planes was divided into a grid measuring 21×21 points (interval 10mm), then the sound intensities on the plane separated from the array plane by 10mm were obtained by the 2 hydrophone method. Measured intensities were described on near-field 3D mapping.⁶⁾ Thus the total radiation power of the array was obtained.

The measurement was conducted for the 3 array patterns shown on Fig.6. Variation of phase and amplitude, frequency of 15kHz and 20kHz were applied for measuring each array pattern.

5. RESULTS AND DISCUSSION

Figure 7 shows the total radiated power output from the array of mode patterns shown on Fig.6 in which the shaded portions are phase shifted from 0° to -180° continuously. The power is normalized by their maximum value. The total power output effect caused by a phase shifted element decreases as the phase degrees increases. Power reductions of all pattern modes for $f=15\text{kHz}$ are larger than those of $f=20\text{kHz}$'s. This is the mutual radiation impedance effect. It increases at lower frequencies.

Figure 8 (a) and (b) are the near-field 3D mappings of the active intensity for $f=15\text{kHz}$ and $f=20\text{kHz}$. At

THE MUTUAL RADIATION IMPEDANCE EFFECT ON PHASED ARRAY

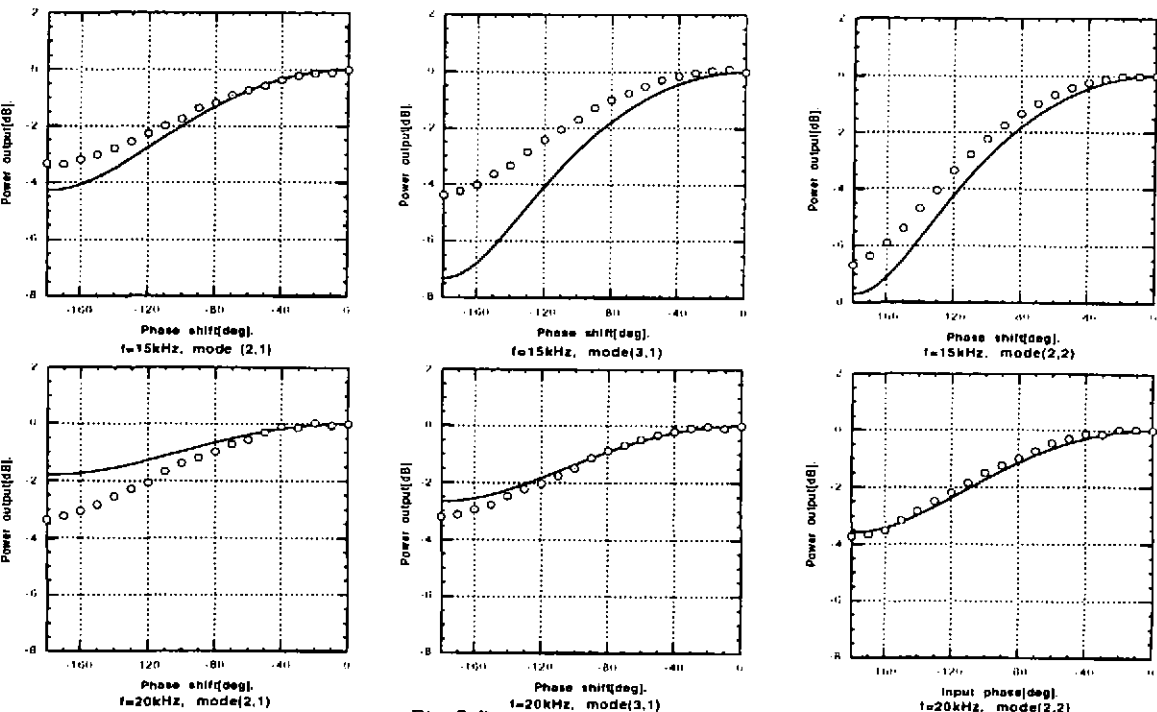


Fig.7 Power output vs phase shift.

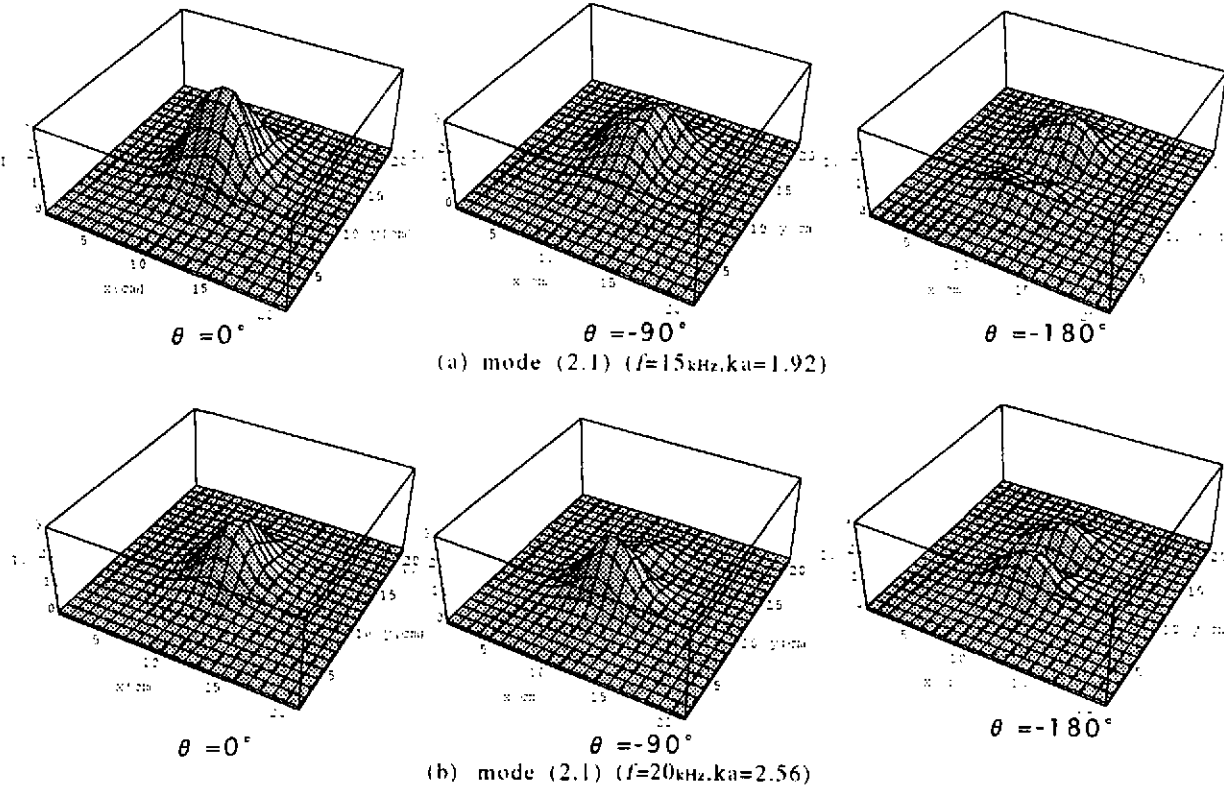


Fig.8 Near-field 3D mapping of real power output from the phased array.

THE MUTUAL RADIATION IMPEDANCE EFFECT ON PHASED ARRAY

$\theta = 0^\circ$ each element is vibrating in an equal phase. The power output character is visualized as if it was one rectangular element. However, at $\theta = -90^\circ$ one element is reducing the power output of another element. Furthermore, at $\theta = -180^\circ$ each element radiates its power individually.

Figure 9 shows near-field 3D mapping of active intensity I and reactive intensity Q for mode (2,2) at $f=20\text{kHz}$. As for the mapping of I , (except for the case of $\theta = -180^\circ$), it is impossible to distinguish the sound source. However, for the Q mappings, the sound source is clearly localized. Especially at $\theta = 0^\circ$, the mapping of I is acting to the sound source, but the mapping of Q shows the vibration of the sound source obviously.

Figure 10 shows the total radiated power output from the array of mode patterns shown in Fig.6 in which the shaded portions' phase is reversed by -180° and the relative velocity amplitude is changed from 0 to 1.5 while non-shaded pistons remain driven at 1.5. The powers are normalized by their maximum values. The total power output from the array becomes a quadratic curve to the velocity amplitude changes of phase reversed elements.⁷⁾ The modes of Fig.6 will be defined as odd-even, odd-odd, and even-even. Generally, the even-even mode pattern gives the most largest reduction.⁸⁾

Output power reduction is caused by the interaction between the elements shown on both phase shifting and velocity amplitude changing patterns. Therefore, considering the mutual radiation impedance should be a requirement for designing the phased array transducer equipment.

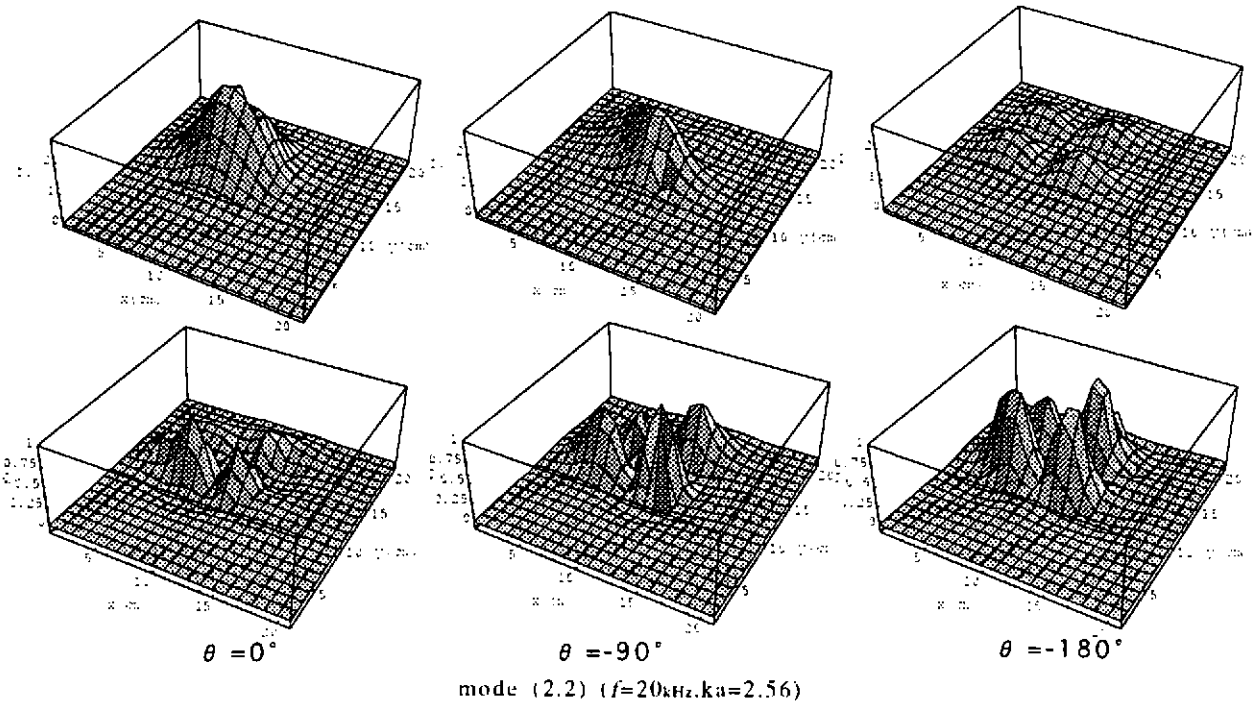


Fig.9 Near-field 3D mapping of active intensity I and reactive intensity Q output from the phased array.

THE MUTUAL RADIATION IMPEDANCE EFFECT ON PHASED ARRAY

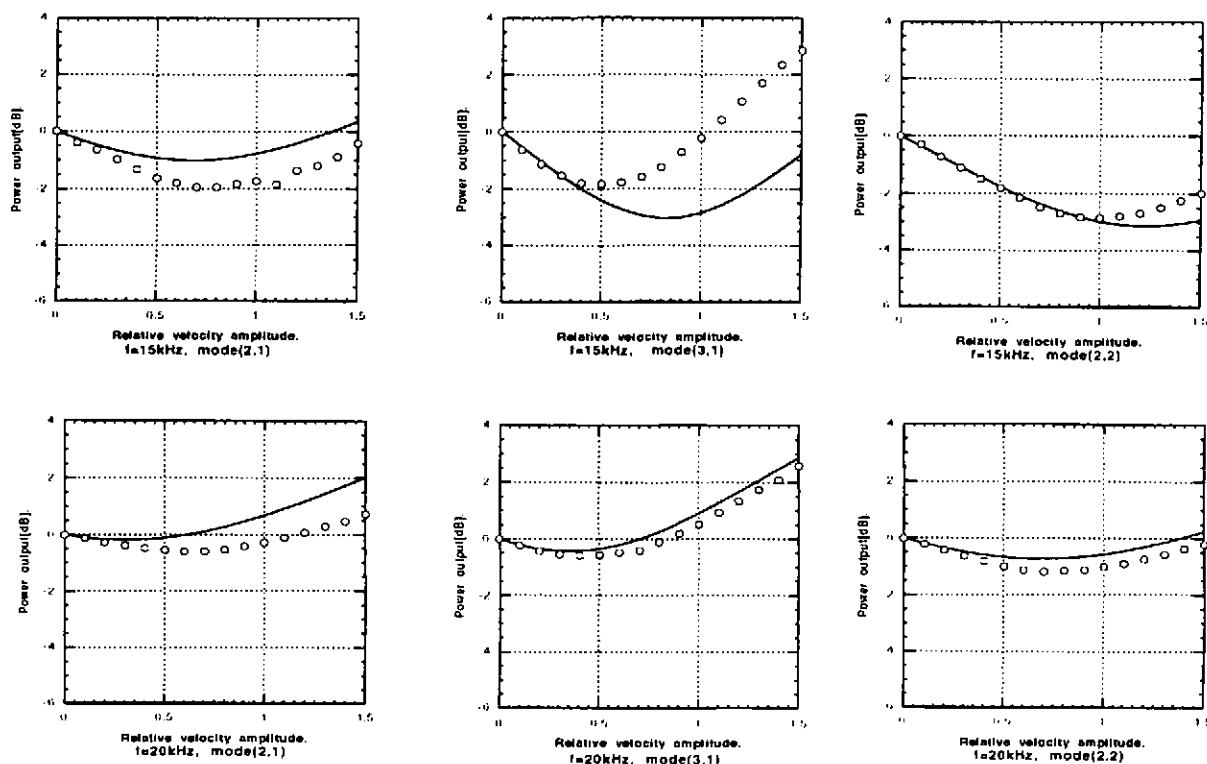


Fig.10 Power output vs relative velocity amplitude.

Both the measured value and the theoretical value became a quadratic curve. The reason for the difference between these values are analyzed in the following two points. One is the influence of the brass baffle board, and the other is the ununiform vibration of the elements. For the former point, the wave length of 15kHz underwater sound is 100mm, while the baffle board, (which is a brass plate), has dimensions of $365 \times 365 \times 10\text{mm}$, therefore, the underwater sound diffraction cannot be avoided. As for the latter point, there must be some ununiformity in mounting the piezo-rubber sheet and in touching the lead wires when molding them by silicon rubber. Therefore, the vibration of each array elements was not equal when they vibrate individually.

The measurement was limited to only 15kHz this time because the lateral oscillation occurred from 10kHz, making lower frequency measurement impossible. This problem may be resolved by using another type of piezoelectric rubber which has a smaller lateral oscillation.

6. CONCLUSION

The power reduction from radiation and the absorption of sound caused by mutual radiation impedance between hydrophone array element at a lower ka region, were tested by a model experiment using a piezoelectric hydrophone array. The basic data for the active acoustic control were provided in this research. It is the existence of the most suitable amplitude velocity for the additional sound source which controls the primary source's power reduction.

THE MUTUAL RADIATION IMPEDANCE EFFECT ON PHASED ARRAY

7. REFERENCES

- [1] R.J.Urick, 'Principles of Underwater Sound for Engineers', McGraw-Hill BookCompay (1967)
- [2] E.M.Arased, 'Mutual Radiation Impedance of Square and Rectangular Pistons in a Rigid Infinite Baffle', *J.Acoust.Soc.Am.*, 36, pp.1521-1525 (1964) .
- [3] C.E.Wallace, 'Radiation Resistance of a Rectangular Panel', *J.Acoust.Soc.Am.*, 51, pp.946-952 (1970) .
- [4] C.Audoly, 'Some aspects of acoustic interaction in sonar transducer arrays', *J.Acoust.Soc.Am.*, 89, pp.1428-1433 (1991) .
- [5] H.Suzuki, 'Mutual Radiation Impedance of a Double-Disk Source and Its Effect on the Radiation Power', *J.Audio.Eng.Soc.*, pp.780-788 (1986) .
- [6] K.Klein and J.Y.Guigne, 'Near-field acoustic intensity mapping using a closed surface', *J.Acoust.Soc.Am.*, 98, pp.973-980 (1995) .
- [7] S.J.Elliott, P.Joseph, P.A.Nelson, and M.E.Jhonson, 'Power output minimization and power absorption in the active control of sound', *J.Acoust.Soc.Am.*, 90, pp.2501-2512 (1991) .
- [8] G.Maidanik, 'Response of Ribbed Panels to Reverberant Acoustic Fields', *J.Acoust.Soc.Am.*, 34, pp.809-826 (1962) .